

## Online measurement of fluence and position for protontherapy beams

C. BENATI<sup>(1)(2)</sup>, A. BORIANO<sup>(1)(2)</sup>, F. BOURHALEB<sup>(3)</sup>, R. CIRIO<sup>(2)(\*)</sup>  
G. A. P. CIRRONE<sup>(4)</sup>, I. CORNELIUS<sup>(2)</sup>, G. CUTTONE<sup>(4)</sup>, M. DONETTI<sup>(2)(5)</sup>  
E. GARELLI<sup>(2)(6)</sup>, S. GIORDANENGO<sup>(2)(\*\*)</sup>, L. GUÉRIN<sup>(7)</sup>, A. LA ROSA<sup>(1)(2)</sup>  
A. LUPARIA<sup>(2)(8)</sup>, F. MARCHETTO<sup>(2)</sup>, F. MARTIN<sup>(7)</sup>, S. MEYRONEINC<sup>(7)</sup>  
C. PERONI<sup>(1)(2)</sup>, G. PITTÀ<sup>(3)</sup>, L. RAFFAELE<sup>(4)(9)</sup>, M. G. SABINI<sup>(4)(10)</sup> and  
L. VALASTRO<sup>(4)(11)</sup>

<sup>(1)</sup> *Dipartimento di Fisica Sperimentale, Università di Torino  
Via Giuria 1, 10125 Torino, Italy*

<sup>(2)</sup> *INFN, Sezione di Torino - Via Giuria 1, 10125 Torino, Italy*

<sup>(3)</sup> *TERA Foundation - Via Puccini 1, 28100 Novara, Italy*

<sup>(4)</sup> *INFN, Laboratori Nazionali del Sud - Via S. Sofia 62, 95100 Catania, Italy*

<sup>(5)</sup> *CNAO Foundation - Via Caminadella 16, 20123 Milano, Italy*

<sup>(6)</sup> *ASP, Viale S. Severo 65, 10133 Torino, Italy*

<sup>(7)</sup> *Institut Curie - Centre de Protontherapie (CPO), Orsay, France*

<sup>(8)</sup> *COREP - C.so Duca Degli Abruzzi 24, 10129 Torino, Italy*

<sup>(9)</sup> *Dipartimento di Radiologia e Radioterapia, Ospedale Universitario  
Via S. Sofia 78, 95100 Catania, Italy*

<sup>(10)</sup> *A.O. Cannizzaro - Via Messina 829, 95126 Catania, Italy*

<sup>(11)</sup> *Dipartimento di Fisica, Università di Torino - Via. S Sofia 64, 95100 Catania, Italy*

(ricevuto il 20 Gennaio 2005)

**Summary.** — Tumour therapy with proton beams has been used for several decades in many centres with very good results in terms of local control and overall survival. Typical pathologies treated with this technique are located in head and neck, eye, prostate and in general at big depths or close to critical organs. The Experimental Physics Department of the University of Turin and the local Section of INFN, in collaboration with INFN Laboratori Nazionali del Sud Catania and Centre de Protontherapie de Orsay Paris, have developed detector systems that allow the measurement of beam position and fluence, obtained in real time during beam delivery. The centre in Catania (CATANA: Centro di AdroTerapia ed Applicazioni Nucleari Avanzate) has been treating patients with eye pathologies since spring 2002 using a superconducting cyclotron accelerating protons up to 62 MeV.

(\*) E-mail: cirio@to.infn.it

(\*\*) Partially supported by Ion Beam Application (IBA), Chemin du Cyclotron 3, B-1348 Louvain-la-Neuve, Belgium.

This kind of treatments need high-resolution monitor systems and for this reason we have developed a 256-strip segmented ionisation chamber, each strip being  $400\ \mu\text{m}$  wide, with a total sensitive area  $13 \times 13\ \text{cm}^2$ . The Centre de Protontherapie de Orsay (CPO) has been operational since 1991 and features a synchrocyclotron used for eye and head and neck tumours with proton beams up to 200 MeV. The monitor system has to work on a large surface and for this purpose we have designed a pixel-segmented ionisation chamber, each pixel being  $5 \times 5\ \text{mm}^2$ , for a total active area of  $16 \times 16\ \text{cm}^2$ . The results obtained with two prototypes of the pixel and strip chambers demonstrate that the detectors allow the measurement of fluence and centre of gravity as requested by clinical specifications.

PACS 87.53.Qc – Proton, neutron, and heavier particle dosimetry: measurements.  
PACS 87.56.Da – Ancillary equipment.

## 1. – Introduction

Proton therapy allows a very precise energy deposition in the tumour while sparing healthy tissue taking advantage of the Bragg peak in the depth dose distribution. A drawback of this technique is the need for complicated apparatuses needed to insure the constant delivery of the therapeutical beam. In particular it is of great importance to continuously measure the beam shape and intensity. Normally the beam shape is measured with 4-sector ionisation chambers, where the information fed back to the control system is up-down and left-right; the fluence measurement is performed with full-area ionisation chambers. To improve such measurements we have developed electrode-segmented ionisation chambers. The two kinds of segmentation (strip or pixel) involve a very different number of electronics channels, as it is intuitive. The choice of one of the two is thus driven by the need for having a faster or slower readout, being this linear with the number of channels.

## 2. – Description of the detectors and the readout electronics

The two detectors are based on the architecture of a parallel-plate ionisation chamber with one of the two electrodes segmented in strips or pixels [1]. Figure 1 shows an exploded view of the chamber used at CATANA. Two anodes, segmented in horizontal and vertical strips, respectively, are mounted facing each other on the two external frames, as schematically shown. Each anode consists of 256 strips each  $400\ \mu\text{m}$  wide, separated by a  $100\ \mu\text{m}$  electrically insulated interspace. The total covered active area is  $(12.8 \times 12.8)\ \text{cm}^2$ , exceeding the typical dimensions of the proton beam. The anodes are made of a  $35\ \mu\text{m}$  thick Kapton foil, covered by a  $15\ \mu\text{m}$  thick aluminium layer. The conducting strips, placed on the aluminised side of the foil, have been obtained by using the standard printed circuit board (PCB) technique. Signals from the strips are brought to four 68 pin connectors located on the edge of the anode frame. The single cathode is sandwiched between the two anodes. It is made by a  $25\ \mu\text{m}$  thick Mylar foil, aluminised on both sides. The thickness of each gas gap is 6 mm, filled with air for the present test. A special effort was taken to minimize the total thickness crossed by the beam; the total water equivalent thickness has been found to be about  $100\ \mu\text{m}$  by measuring the shift in position of the Bragg peak.

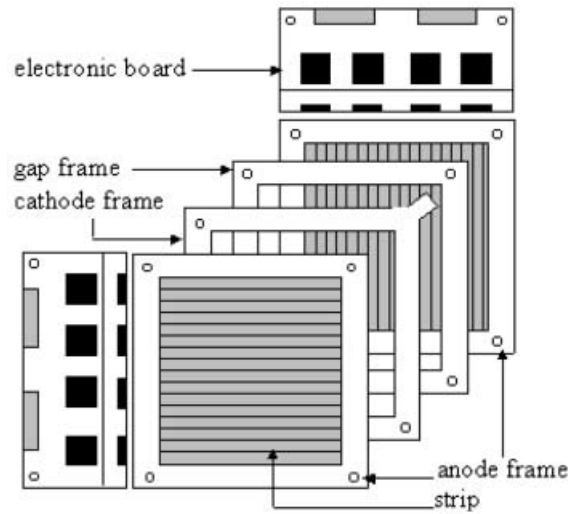
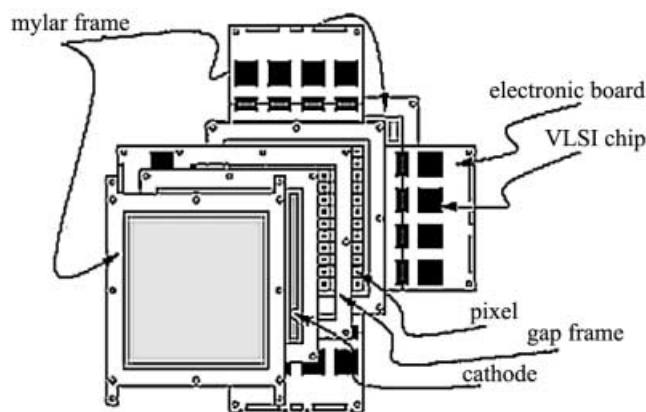


Fig. 1. – Schematic drawing of the strip ionisation chamber tested on the CATANA beam.

In figs. 2 and 3 are shown, respectively, the schematic drawing and a picture of the chamber tested at CPO. The construction details are equal to the strips chambers used at CATANA, the major difference being that the pattern drawn on the anode has pixels instead of strips. There is a total of 1024 pixels, arranged on a  $32 \times 32$  square 16 cm of side; each pixel has a 5 mm side and the interspace between two neighbouring pixels is 0.1 mm. In this case it was not possible to have a single-layer printed circuit board for the anode, as it would have been impossible to bring out the electric signals of the central pixels; thus the anode is made of  $50 \mu\text{m}$  thick Kapton with  $25 \mu\text{m}$  thick copper. The signal of each pixel is brought to the input of the readout electronics through a metallized hole and a copper track that runs on the opposite face of the Kapton.



[A2]

Fig. 2. – Schematic drawing of the pixel ionisation chamber tested on the CPO beam.

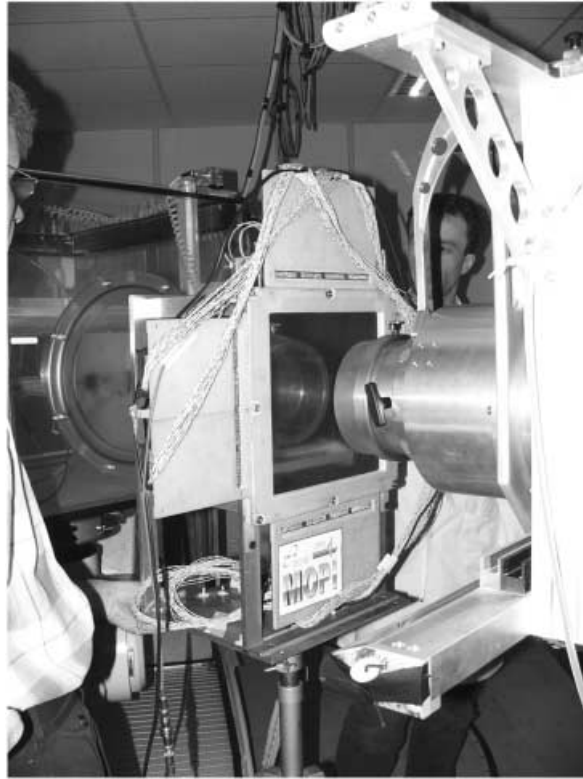


Fig. 3. – Picture of the pixel ionisation chamber on the CPO beam line. The chamber is located at the isocenter, inside the treatment room. One can notice the final collimator on the right side of the picture, reflecting on the chamber's aluminised Mylar cathode.

The electric field is generated by polarizing the cathode Mylar foil. Typically the high-voltage value is set to  $-500$  V. The strip voltage is set to around  $2$  V, the same voltage as the front-end input circuit.

The design of the front end is based on the recycling integrator architecture [2]. Briefly, the input current from each pixel is integrated and a number of pulses proportional to the charge collected by an individual channel is sent to a 16-bit counter. An ensemble of 64 channels has been integrated in a single Very Large Scale Integration (VLSI) chip [3].

At any given time all the counters can be latched and the results are stored in a register. This is like taking a snapshot of the collected charges. The relevant features of the front-end circuit are summarized below:

- the charge corresponding to a pulse (charge quantum) can be adjusted between  $100$  fC and  $800$  fC via an externally regulated voltage;
- maximum pulse frequency is  $5$  MHz which results in a limit for the input current of  $4$   $\mu$ A for a charge quantum set at  $800$  fC;
- linearity from  $100$  pA up to the maximum current is within 1%;
- dark current counting rate is at the level of  $\sim 1$  Hz;

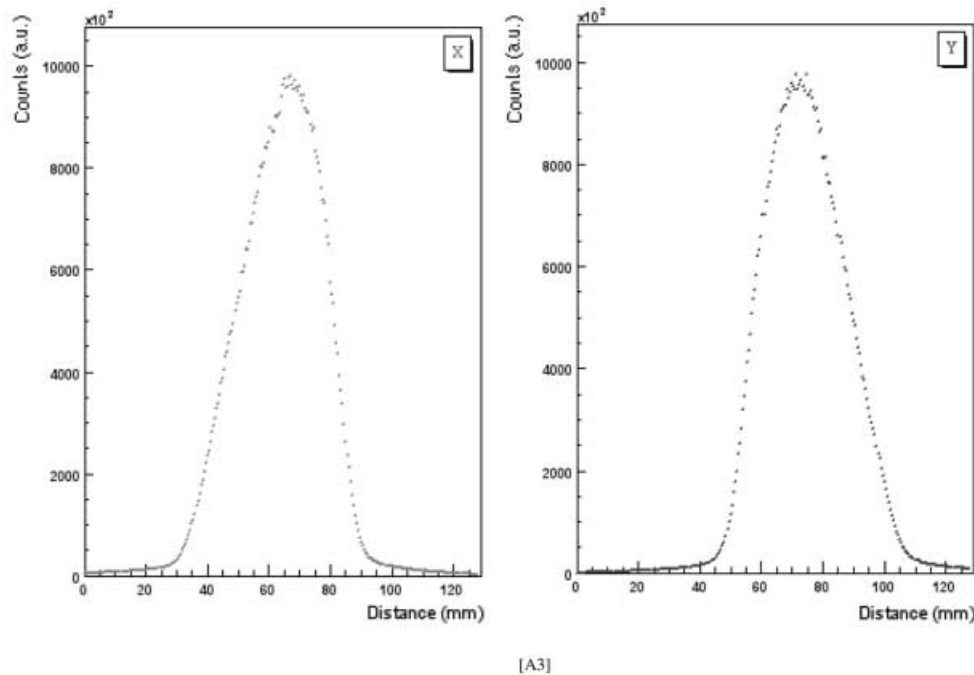


Fig. 4. – Projections of the CATANA beam on the vertical (X) and horizontal (Y) axis.

- charge quantum spread is less than 1%;
- the change of charge quantum as a function of temperature in the range 20–30 °C is less than 1 fC/°C for a charge quantum set at 600 fC;
- no dead time is introduced due to readout, because the latch located at the output of the counters does not affect the counting itself.

Each of the two CATANA chambers has a total of 256 channels and is read out with one custom printed circuit board that houses four VLSI chips and all the electronics needed to receive and send the digital signals to the computer that can be located at a maximum distance of 200 meters from the chamber; the CPO chamber needs 4 such boards.

Data acquisition was performed using a commercial input/output register read out by a Personal Computer running National Instrument LabView software. The readout rate can be as high as 1kHz; in these preliminary tests the readout rate of the whole detector was set at 5 Hz at CATANA and 10 Hz at CPO.

### 3. – Experimental set-up

The two detector prototypes have been tested on the CATANA and CPO beam lines. In the former, the 62 MeV proton beam from the superconducting cyclotron operating at the Laboratori Nazionali del Sud of INFN (Catania) exits in air through a 50  $\mu\text{m}$  Kapton window placed at about 3 meters from the isocenter. A first 15  $\mu\text{m}$  tantalum scattering

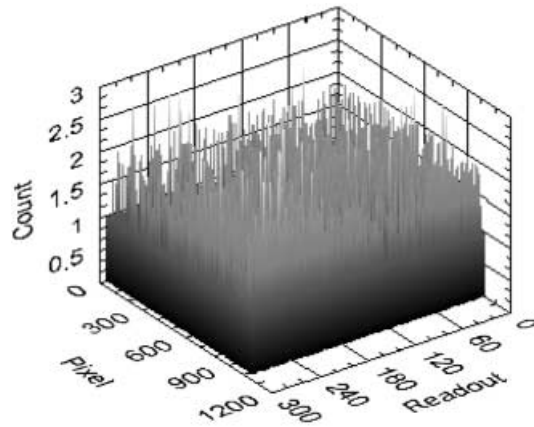


Fig. 5. – Pedestals measured with the pixel ionisation chamber in the CPO treatment room. On the “Pixel” axis the 1024 pixels are shown, whereas the “Readout” axis runs from 0 to 300, the number of acquisitions taken every 100 ms in a 30 s run.

foil is placed upstream of the window in vacuum, followed by a second  $25\ \mu\text{m}$  tantalum foil provided with a central brass stopper of 4 mm in diameter, 7 mm thick and placed in air. The double-foil scattering system is optimised to obtain a good homogeneity in terms of lateral dose distribution, minimizing the energy loss. The range shifter and range modulator are mounted in two different boxes downstream of the scattering system. Two transmission monitor chambers, used for on-line control of the dose delivered to the patients during treatment, are placed further down along the beam line followed by the strip ionisation chambers. The nozzle, a 37 cm long brass cylinder with a 45 mm hole, terminates with the final collimator (25 mm in diameter for the reference measures). The

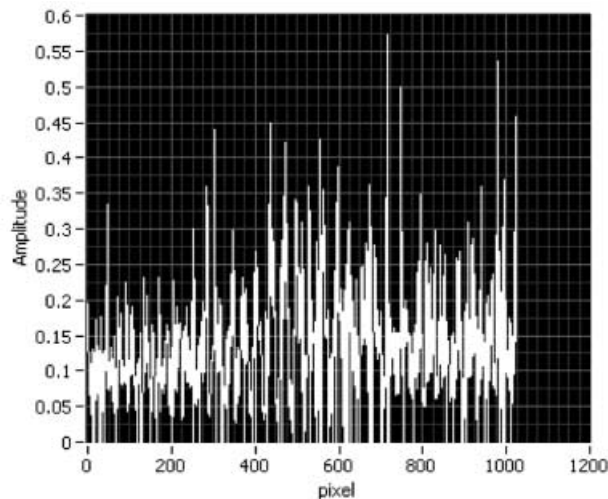


Fig. 6. – Standard deviation of the pedestals measured on each of the 1024 pixels in 5 subsequent runs at CPO.

TABLE I. – *The linearity of response of the pixel ionisation chamber versus dose has been measured at CPO with 4 different doses (Monitor Units, MU). The experimental column shows the average on 3 subsequent runs of the response of 16 central pixels,  $\sigma$  being the standard deviation. In the last two columns the result of the linear fit and the difference between fitted and experimental are listed.*

MU	Experimental	$\sigma$ (%)	Fit	Difference (%)
1	4631.9	2.45	4615.7	0.351
10	44421.3	0.12	44427.3	0.014
50	221630.1	0.23	221367.6	0.119
100	442241.7	0.21	442543.0	0.068

final collimator is located 8 cm upstream of the isocenter, where a diode beam scanning system is placed for off-line beam profile measurements.

The beam line used at CPO is indeed very similar to the one found at CATANA, although it is designed for a higher-energy beam and for the treatment of larger size tumors. The major difference in the two test set-ups was that at CPO the pixel ionisation chamber was placed at the isocenter, inside the treatment room; this allowed an easier access with respect to when the chamber would have been placed along the beam line. Moreover, the pixel chamber tested at CPO was slightly different from the final one, described above; it had 7.5 mm side pixels for a total active area of  $24 \times 24$  cm<sup>2</sup>.

#### 4. – Experimental results

In both tests the goal was to verify that the detectors were able to measure the beam shape and fluence with minimum noise and good stability.

At CATANA data were taken in 15 runs of 30 s, reading out the strip ionisation chamber at a rate of 5 Hz and the CATANA ionisation monitor chambers. The typical beam current was 2.5 nA. The detectors results for the integrated beam fluence agree within 0.4%. In fig. 4 the horizontal and vertical projections of the beam profile are shown; indeed the large number of strips permits to reach a high spatial resolution allowing the measurement of very small modifications in the beam shape. A quantitative measurement of this sensitivity will be performed in the following months. So far the skewness, defined as  $\gamma = \mu_3/\sigma^3$  with  $\mu_3 = \frac{\sum_i (x_i - \mu)^3 c_i}{\sum_i c_i}$  and  $\sigma = \sqrt{\frac{\sum_i (x_i - \mu)^2 c_i}{\sum_i c_i}}$ , has been measured for extreme values of the setting of tuning magnets placed along the beam line. The relative variation  $\Delta\gamma/\gamma$  is around 0.5%.

In the CPO tests the attention was driven by noise, linearity *versus* dose and stability of response. The count rate of the chamber with no beam (pedestals) was measured in 5 different runs of 30 seconds each. As showed in fig. 5, for each reading of the chamber the single pixel does not read more than 2 counts, while the counting frequency (mean count per second) has a mean of about 4-5 count/s, a max value of 16 count/s and a standard deviation equal to 2.4 count/s. The standard deviation calculated on the 5 runs is shown in fig. 6; it features a mean value of about 0.1 counts/s, which demonstrates the good stability of the pixel chamber in the pedestal measure. The linearity of response as a function of the total dose has been measured irradiating the chamber with 4 different

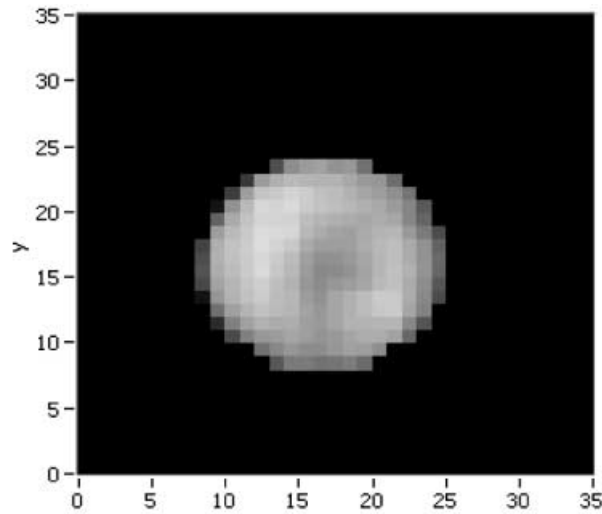


Fig. 7. – Shape of the CPO beam used for the reproducibility tests as reconstructed by the pixel ionisation chamber.

dose values. The shape of the beam, kept constant for the 4 irradiations, was a circle 15 cm in diameter. The total dose was measured in two ways: summing the counts of the  $4 \times 4$  central pixels and summing the counts of the whole chamber. In both cases the pedestals have been subtracted. Both methods resulted equivalent inside the experimental uncertainty of 0.2%. The results of the linear fit are shown in table I, where the difference between fit and experimental value is below 0.35%. The very high error (2.45%) obtained for the 1 Monitor Unit measurement has been caused by the uncertainty of the accelerator system in delivering such small dose. The stability of response has been measured irradiating the chamber with 100 MU of a circular shaped beam (a typical run is shown in fig. 7) and comparing the relative response of each pixel along 10 runs. The standard deviation of the relative gain variation was below 0.5%.

## 5. – Conclusions

Two detector systems have been built with the goal of measuring in real time the fluence and the shape of proton beams used for radiotherapy. They have been tested in operating conditions on the beam lines of CATANA (at LNS-INFN) and CPO. The results show that noise, stability of response, linearity *versus* dose and sensitivity to beam shape variation are adequate. At present both detectors are being installed in permanent positions along the beam lines to be routinely used during patient treatment.

## REFERENCES

- [1] BONIN R. *et al.*, *Nucl. Instrum. Methods Phys. Res. A*, **519** (2004) 674.
- [2] GOTTSCHALK B., *Nucl. Instrum. Methods Phys. Res. A*, **207** (1983) 417.
- [3] BONAZZOLA G. C. *et al.*, *Nucl. Instrum. Methods Phys. Res. A*, **405** (1998) 111.